The effect of impurities on the R-point instability in $KMnF_3$. II. A neutron scattering study

1989 J. Phys.: Condens. Matter 1 3579

(http://iopscience.iop.org/0953-8984/1/23/003)

J. Phys.: Condens. Matter 1 (1989) 3579–3589. Printed in the UK

The effect of impurities on the R-point instability in $KMnF_3$: II. A neutron scattering study

U J Cox† and L D Cussen‡
Department of Physics, University of Edinburgh, Mayfield Road, Edinburgh, Scotland

Received 1 September 1988

Abstract. The frequency dependence of the critical fluctuations at the antiferrodistortive phase transition exhibited by the disordered crystals $KMn_{0.99}Mg_{0.01}F_3$ and $KMn_{0.9}Mg_{0.1}F_3$ has been studied using neutron scattering techniques. In pure $KMnF_3$ the soft R_{25} mode is overdamped for temperatures below $\sim(T_c + 40)$ K. A similar behaviour is observed in the disordered crystals, but the damping constant is increased by the presence of the impurities. The amplitude of the central peak observed in the spectral response for pure $KMnF_3$ is not significantly increased by the addition of the impurities. This is consistent with measurements of the anomalous component observed close to T_c in complimentary x-ray scattering studies, which showed that this component was reduced by the addition of impurities. The results further indicate that although the temperature dependence of the anomalous scattering is similar in both the x-ray and neutron scattering experiments, the neutron central peak persists over the temperature range T_c to $(T_c + 20)$ K while the x-ray anomaly was only observed for a few degrees above T_c. Thus, while the anomalous scattering measured using the two techniques is related to the impurity concentration in the disordered crystals, the two features must be to some extent distinct.

1. Introduction

Much experimental and theoretical effort has been devoted to understanding the frequency dependence of the critical fluctuations above the cubic–tetragonal phase transition in perovskite crystals, and in particular to explain the origin of the quasi-elastic scattering or 'central peak' (see Bruce and Cowley 1980 for a review). One approach, described by Halperin and Varma (1976), considers the influence of crystal imperfections upon the static and dynamic critical response at a displacive structural phase transition. This predicts that an impurity frozen in a symmetry-breaking position will couple linearly to the order parameter and induce a non-zero value of the order parameter in the neighbourhood of the impurity, even above the transition temperature, which will give rise to an elastic scattering peak. Neutron scattering experiments have been performed on hydrogen-reduced $SrTiO_3$ in an attempt to quantify the role of defects at a structural phase transition (Hastings *et al* 1978), but the effect of impurities on such a transition is still an unresolved problem. This paper describes the influence of substitutional impurities upon the structural phase transition in $KMnF_3$ by means of inelastic neutron scattering measurements and, in conjunction with the companion paper describing x-ray studies

† Present address: Department of Physics, University of Durham, Durham, UK.
‡ Present address: Institut Laue-Langevin, 38042 Grenoble Cédex, France.

0953-8984/89/233579 + 11 $02.50

on the same crystals (Cox 1989, hereafter referred to as I), investigates the relationship between the central peak and the anomalous component observed in x-ray scattering experiments.

2. Experimental arrangement

The neutron scattering experiments were performed on the IN3 triple axis spectrometer situated on the guide tube of the nuclear reactor at the Institut Laue–Langevin, Grenoble, France. The monochromator was a bent pyrolitic graphite crystal, and the analyser a flat germanium crystal. Soller slit systems with horizontal divergence 20′ – 20′ – 30′ were used to define the neutron path. The vertical divergence was determined by the natural collimator heights and the size of the crystal to be ~3°. Two different incident neutron energies were used to produce two arrangements of differing resolution. The first was achieved with a pre-sample pyrolytic graphite filter which fixed the incident energy at 3.52 THz and gave an energy resolution of 0.12 THz. ((Full width at half maximum (FWHM), isotropic scattering). The second was achieved with a pre-sample cooled beryllium filter, which fixed the incident energy at 1.12 THz and gave an energy resolution of 0.02 THz (FWHM, isotropic scattering). Second-order contamination was eliminated with the use of a germanium analyser crystal.

3. Sample preparation

The two samples consisted of the remainder of the crystals $KMn_{0.99}Mg_{0.01}F_3$ and $KMn_{0.9}Mg_{0.1}F_3$ grown by Dr R C C Ward (Crystal Growth Facility, University of Oxford) after removal of the slices for the x-ray work. The $KMn_{0.99}Mg_{0.01}F_3$ sample had a volume of ~0.5 cm^3 and a rather poor mosaic spread of 0.7(1)°, and the $KMn_{0.9}Mg_{0.1}F_3$ sample a volume of ~1.3 cm^3 and a mosaic spread of 0.20(5)°. Each sample was mounted in turn in a cryostat which had a temperature stability of ±0.05 K and aligned with a [1–10] axis vertical.

4. Experimental results

4.1. Measurement of T_c

The transition temperature in the disordered crystals was measured using neutron scattering by monitoring the peak intensity at the zone-boundary reciprocal lattice point (0.5 0.5 1.5) as the temperature was lowered through the transition. The results for the two samples are shown in figure 1, and give values for $T_c^1 = (184 \pm 1)$ K and $T_c^{10} = (162 \pm 1)$ K, which are in agreement with the values for the transition temperatures determined using x-ray scattering (see I).

4.2. Critical scattering

4.2.1. Experimental measurements. The energy dependence of the critical scattering above T_c was measured at (0.5 0.5 1.5) using incident neutron energies of 3.52 and 1.12 THz for both disordered crystals. Some high resolution measurements on pure

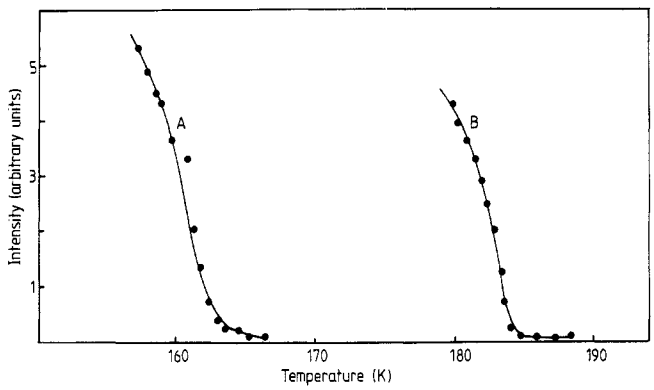

Figure 1. The peak intensity of the neutron scattering (normalised to a monitor count of 3) at the reciprocal lattice point (0.5 0.5 1.5) obtained with an incident energy of 1.12 THz for the disordered crystals $KMn_{1-x}Mg_xF_3$ ($x > 0$) as each sample was cooled through the transition. Curve A, $x = 0.1$; curve B, $x = 0.01$.

$KMnF_3$ (the same sample as used in the x-ray experiments described by Nicholls and Cowley (1987)) were also made. Previous measurements of the response function of the soft R_{25} mode in $KMnF_3$ by Gesi *et al* (1972) and Shapiro *et al* (1972) and in $LaAlO_3$ by Kjems *et al* (1973) have shown that the energy resolution achieved with an incident neutron energy of 3.52 THz is insufficient to resolve a central peak from an overdamped phonon, and that the higher resolution obtained with an incident neutron energy of 1.12 THz is necessary for such a distinction to be made. This was also the case for measurements of the response function in $KMn_{0.99}Mg_{0.01}F_3$ and $KMn_{0.9}Mg_{0.1}F_3$ at all temperatures investigated above T_c, though the problem was further aggravated because the larger damping constant in these crystals meant the overdamped phonon was more narrow than in $KMnF_3$. The results are illustrated in figure 2, which shows high resolution measurements of the response function in $KMnF_3$, $KMn_{0.99}Mg_{0.01}F_3$ and $KMn_{0.9}Mg_{0.1}F_3$ at approximately the same reduced temperature $t = (T - T_c)/T_c \sim 0.033$. The counting time for these data was extremely long, in an attempt to distinguish the phonon from a uniform background. Qualitatively, the scattering profile in $KMnF_3$ is more consistent with a separation into two components (a broad overdamped phonon centered on zero frequency, together with a narrow central peak superimposed) than the scattering profile in the disordered crystals. This problem is reflected in the analysis of the lower resolution data for the disordered crystals, where reasonable fits were obtained for zero central peak, and where inclusion of a central peak did not affect the width of the phonon very significantly. The results from the analysis are discussed in § 5.

The widths and peak heights of the critical scattering measured in the disordered crystals with an incident neutron energy of 3.52 THz are shown in figures 3 (with differing vertical scales for the two samples) and 4 as functions of temperature (triangles); the full curves are guides to the eye. In all cases a small amount of incoherent scattering background was subtracted from the data. In $KMn_{0.99}Mg_{0.01}F_3$ the width decreases approximately linearly with decreasing temperature, while the peak intensity increases exponentially. In $KMn_{0.9}Mg_{0.1}F_3$ the width of the scattering is considerably narrower than in $KMn_{0.99}Mg_{0.01}F_3$, and less temperature dependent, beginning to saturate as T_c is approached. The amplitude of the scattering is more intense in $KMn_{0.9}Mg_{0.01}F_3$ because

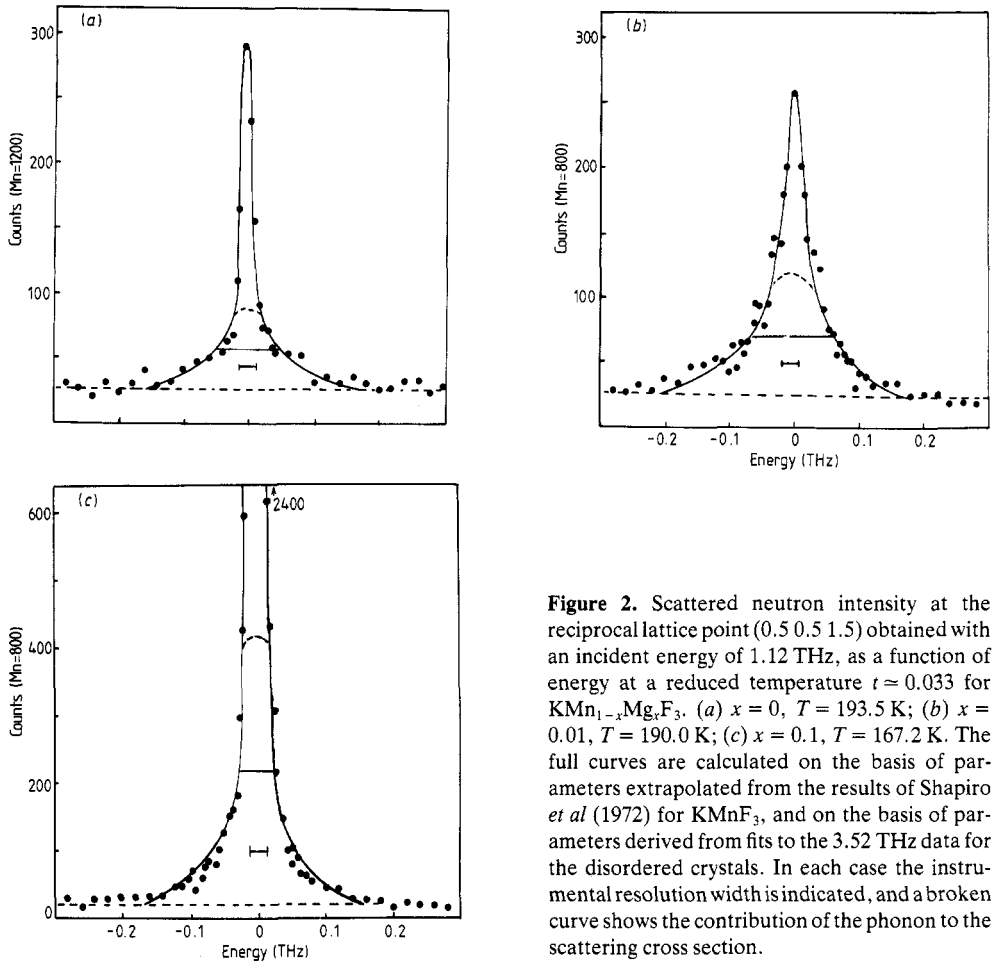

Figure 2. Scattered neutron intensity at the reciprocal lattice point (0.5 0.5 1.5) obtained with an incident energy of 1.12 THz, as a function of energy at a reduced temperature $t \simeq 0.033$ for $KMn_{1-x}Mg_xF_3$. (*a*) $x = 0$, $T = 193.5$ K; (*b*) $x = 0.01$, $T = 190.0$ K; (*c*) $x = 0.1$, $T = 167.2$ K. The full curves are calculated on the basis of parameters extrapolated from the results of Shapiro *et al* (1972) for $KMnF_3$, and on the basis of parameters derived from fits to the 3.52 THz data for the disordered crystals. In each case the instrumental resolution width is indicated, and a broken curve shows the contribution of the phonon to the scattering cross section.

of the larger sample volume, but the temperature dependence of the peak intensity is nominally the same in the two samples.

The widths of the scattering obtained in the two crystals with an incident neutron energy of 1.12 THz are also shown as functions of temperature in figure 3 (crosses). In these measurements, the phonon was indistinguishable from a uniform background that is above the level of incoherence, and has been subtracted out. The measured widths are independent of temperature at a value consistent with the resolution, which suggests that the scattering is a resolution-limited central peak. The inverse peak intensity of this scattering in the three compounds is shown in figure 5 as a function of reduced temperature. The graph shows that for $t > 0.03$, the gradient of the three data sets is nominally the same. The magnitude of the central peak in the three samples can be roughly compared if the sample volume is taken into account. When this is done, the central peak intensity is still greatest in $KMn_{0.9}Mg_{0.1}F_3$, but is smaller in $KMn_{0.99}Mg_{0.01}F_3$ than in pure $KMnF_3$. These results are discussed in § 5.

4.2.2. Analysis of results. The critical scattering data collected above T_c in $KMn_{0.99}Mg_{0.01}F_3$ and $KMn_{0.9}Mg_{0.1}F_3$ with an incident neutron energy of 3.52 THz was

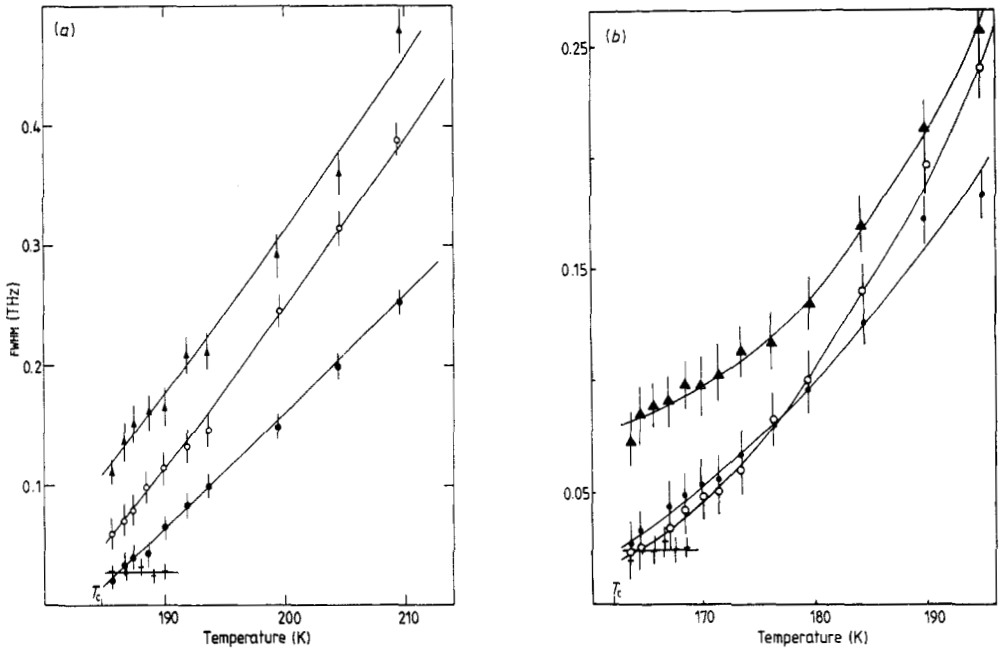

Figure 3. The energy width (full width at half maximum) of the neutron scattering at the reciprocal lattice point (0.5 0.5 1.5) for $KMn_{1-x}Mg_xF_3$ as a function of temperature. (*a*) $x = 0.01$, (*b*) $x = 0.1$. ▲, + refer to the widths of the unprocessed experimental data, ▲ to those collected with an incident energy of 3.52 THz, and + to an incident energy of 1.12 THz. ○ correspond to the width of the phonon obtained when the data was fitted to the model described in § 4.2.2 with a non-zero central peak, and ● to the width of the phonon obtained when the central peak was constrained to be zero.

analysed by a least squares fit to a trial function $I(\boldsymbol{q}, \omega)$, where $I(\boldsymbol{q}, \omega)$ is the convolution of a model scattering function $S(\boldsymbol{q}, \omega)$ with the instrumental response function

$$I(\boldsymbol{q}, \omega) = \frac{k_f}{k_i} \int\int S(\boldsymbol{q}, \omega) R(\boldsymbol{q}' - \boldsymbol{q}, \omega' - \omega)\, \mathrm{d}\boldsymbol{q}'\, \mathrm{d}\omega' \tag{1}$$

The model $S(\boldsymbol{q}, \omega)$ used here was the phenomenological model assumed by Shapiro *et al* (1972) in their analysis of the critical scattering measured above T_c in $SrTiO_3$. They supposed that the response function was that of a damped simple harmonic oscillator coupled, with a constant δ, to an unspecified internal degree of freedom. The latter provides an additional channel for decay for phonon fluctuations with frequencies ω less than a characteristic frequency γ. The scattering function can be split into two terms if the damping constant $\Gamma_0 \ll \delta^2/\gamma$ and the frequency $\omega_\infty \gg \gamma$, using

$$S(\boldsymbol{q}, \omega) = S_{ph}(\boldsymbol{q}, \omega) + S_{ce}(\boldsymbol{q}, \omega) \tag{2}$$

where

$$S_{ph}(\boldsymbol{q}, \omega) = [|F(\boldsymbol{\tau}_R)|^2 k_B T/\pi]\{\Gamma_0/[\omega_\infty^2(\boldsymbol{q}, T) - \omega^2]^2 + \omega^2 \Gamma_0^2\} \tag{3}$$

is the damped harmonic oscillator response with characteristic frequencies $\pm\omega_\infty(\boldsymbol{q}, T)$ in the high temperature limit with $F(\boldsymbol{\tau}_R)$ the structure factor at the R-point, and

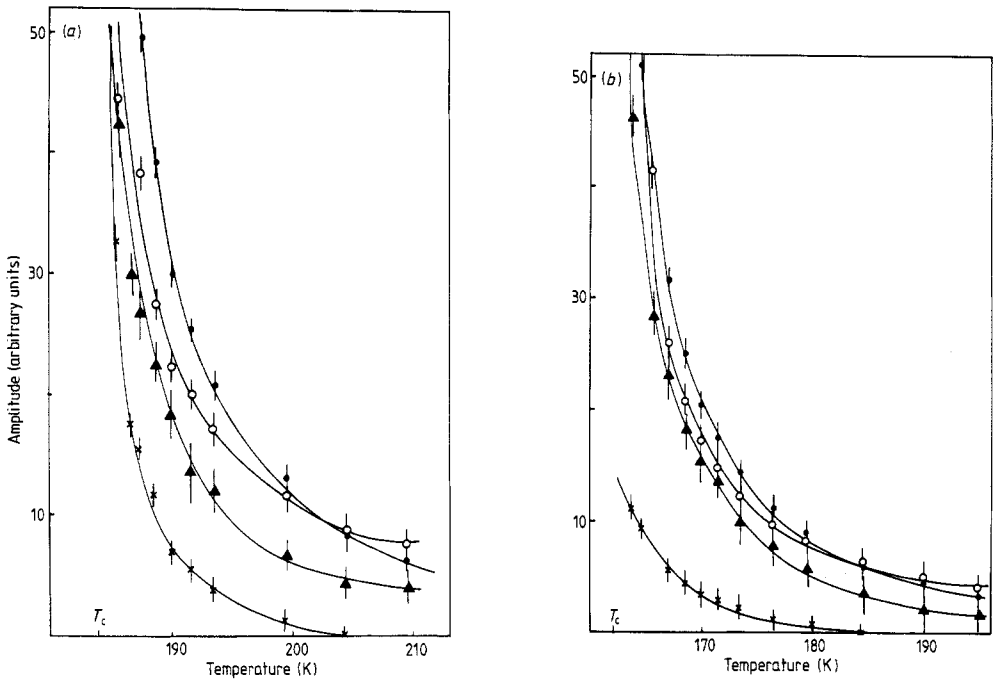

Figure 4. The amplitude of the neutron scattering at the reciprocal lattice point (0.5 0.5 1.5) for $KMn_{1-x}Mg_xF_3$ as a function of temperature for (*a*) $x = 0.01$ and (*b*) $x = 0.1$. ▲ refer to the peak intensity of the unprocessed experimental data collected with an incident energy of 3.52 THz and normalised to a monitor count of 12. ○, + correspond to the amplitudes of the phonon and central peaks obtained when the data was fitted to the model described in § 4.2.2 with a non-zero central peak, ○ to the amplitude of the phonon and + to the amplitude of the central peak. ● refer to the amplitude of the phonon obtained when the central peak was constrained to be zero.

$$S_{ce}(\boldsymbol{q}, \omega) = [|F(\boldsymbol{\tau}_R)|^2 k_B T/\pi][\delta^2(T)/\omega_0^2(\boldsymbol{q}, T)\omega_\infty^2(\boldsymbol{q}, T)][\gamma'/(\omega^2 + \gamma'^2)] \tag{4}$$

is a narrow Lorentzian of width $\gamma' = \gamma(\omega_0^2/\omega_\infty^2)$ centred about $\omega = 0$. The scattering function obeys the sum rule

$$\int_{-\infty}^{+\infty} S(\boldsymbol{q}, \omega)\, \mathrm{d}\omega = [k_B T |F(\boldsymbol{\tau}_R)|^2/\omega_0^2(\boldsymbol{q}, T)] \tag{5}$$

where $\omega_0^2(\boldsymbol{q}, T) = \omega_\infty^2(\boldsymbol{q}, T) - \delta^2(T)$ is the square of the renormalised mode frequency in the limit as ω tends to zero.

In the fitting it was assumed that Γ_0, γ' and δ were all independent of wavevector, so the entire q-dependence of $S(\boldsymbol{q}, \omega)$ was included in the phonon frequency $\omega_\infty(\boldsymbol{q}, T)$. The phonon dispersion close to the R-point in $KMnF_3$ is

$$[\omega_\infty^2(\boldsymbol{q}, T)]_{ij} = [\omega_\infty^2(0, T) + \lambda(\boldsymbol{q}^2 + f\boldsymbol{q}_i^2)]\delta_{ij} + h\boldsymbol{q}_i \cdot \boldsymbol{q}_j(1 - \delta_{ij}). \tag{6}$$

As in the analysis of the x-ray data described in I, the off-diagonal elements of the dynamical matrix were neglected (that is, $h = 0$), and the anisotropy parameter f was fixed at -1. The parameter λ was constrained to equal 41 THz^2 $Å^2$ (measured at $T =$ 295 K by Gesi *et al* (1972)). Detailed knowledge of the dispersion near the R-point at temperatures closer to T_c is not experimentally accessible because the phonon is

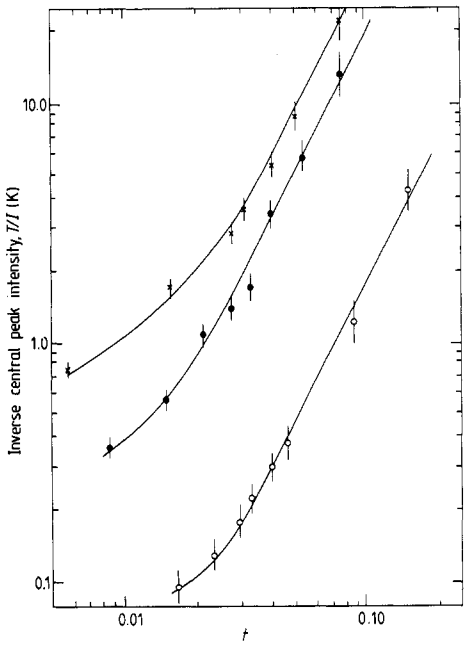

Figure 5. Temperature over the observed peak intensity of the central component (normalised to a monitor count of 300) at the reciprocal lattice point (0.5 0.5 1.5) for $KMn_{1-x}Mg_xF_3$. +, $x = 0$; ●, $x = 0.01$; ○, $x = 0.1$.

overdamped. This means that the information extracted from the results of the data analysis will have an inherent error. The width γ' of the central peak was chosen to be such that it was always smaller than the energy resolution of the spectrometer.

The overdamped soft-phonon also means that the fitting of data is hindered by the difficulty in determining an unambiguous value for the overall scale. This problem was tackled for each sample in the following way. An energy scan collected at the R-point at a temperature well above the transition was chosen, and the frequency $\omega_\infty(0, T)$ and damping constant Γ_0 were fixed at the values found by previous measurements (chiefly those of Gesi *et al* 1972); the central peak amplitude δ was held at zero. The scaling parameter was then allowed to converge to its optimum. The value was fixed for all scans, and the parameters $\omega_\infty(0, T)$ and Γ_0 allowed to vary. After the phonon parameters had been determined, $\delta(T)$ was allowed to vary to fit the central peak. The parameters obtained for a reduced temperature $t \sim 0.033$ in $KMn_{0.99}Mg_{0.01}F_3$ and $KMn_{0.9}Mg_{0.1}F_3$ (except for a scaling parameter) were used to draw the full curves through the higher-resolution data shown in figure 2(*b*) and 2(*c*), where the contribution of the phonon is indicated by the broken curve. For figure 2(*a*), parameters extrapolated from the results of Shapiro *et al* (1972) were used.

In both disordered crystals reasonable fits were achieved with either a zero or a non-zero value for δ, and so results for the two cases are discussed. For an overdamped phonon, $S_{ph}(\boldsymbol{q}, \omega)$ is an anisotropic Lorentzian with an energy width $\omega_{ph}(\boldsymbol{q}, T) = \omega_\infty^2(\boldsymbol{q}, T)/\Gamma_0$ centred on zero frequency, and so this parameter is used to represent the analysed data. Figure 3 shows the obtained values of $2\omega_{ph}(0, T)$ as a function of temperature for the disordered crystals; the solid curves are guides to the eye. The contributions of the phonon and central peak to the scattering amplitude are given by the

sum rule, and are shown in figure 4 as a function of temperature for the two crystals; the solid curves are again guides to the eye. These results will now be discussed.

5. Discussion of results

5.1. Critical scattering

When a non-zero value of δ was incorporated into the fit, the values of $\omega_{ph}(0, T)$ achieved for $KMn_{0.99}Mg_{0.01}F_3$ were consistently greater than those obtained with $\delta = 0$, as would be expected. This included a decrease in the damping constant Γ_0 from 1.10(15) THz to 0.75(5) THz, which was independent of temperature in both fits. As the damping constant has been measured by Gesi *et al* (1972) to be 0.84(2) THz in $KMnF_3$, both these values are consistent, though it is expected that if impurities are introduced into a system the damping would increase rather than decrease. The measurements with the higher resolution suggest that a central peak is present in the response function, with an intensity which decreases rapidly as T_c is approached. A similar temperature dependence is indicated by analysis of the data, which also shows that the central peak is not the major part of the integrated scattering at any temperature.

In $KMn_{0.9}Mg_{0.1}F_3$, the values of $\omega_{ph}(0, T)$ obtained from the fits with $\delta = 0$ are hardly changed when a central peak is included. This is mainly because of the difficulty in separating the cross section into two components when the phonon is very narrow, and suggests that any central peak is small. However, when a central peak was included the damping constant became less temperature dependent (with $\delta = 0$ the damping decreased with decreasing values of reduced temperature) with an average of 2.2(3) THz. The measurements with the higher resolution indicate that the response function contains a significant central peak, but data analysis finds the contribution of the central peak to the integrated scattering to be much less than that of the softening phonon. We therefore conclude that there is some ambiguity in the results for $KMn_{0.9}Mg_{0.1}F_3$, but that the central peak is not significantly enhanced over that measured in pure $KMnF_3$.

The temperature dependence of the peak intensity of the central component in pure and disordered $KMnF_3$ is well described by $I_{ce}(T) \sim T/(T - T_c)^2$ for $t > 0.03$. This is consistent with equation (4) for $\omega_\infty^2(T) \gg \delta^2(T)$, which gives

$$S_{ce}(q = 0, \omega = (0, T)) \sim T\delta^2(T)/\omega_\infty^4(0, T). \tag{7}$$

The results of the analysis of the critical scattering measured in the disordered crystals gave $\delta(T)$ to be approximately constant and the soft-mode frequency $\omega_\infty^2(0, T) \simeq (T - T_c)$ for $T \gg T_c$. For temperatures closer to T_c, the amplitude of the central peak increases less rapidly in all three samples than equation (7) suggests.

5.2. The effect of impurities on the central peak in $KMnF_3$

To date, all measurements of the energy width of the central peak observed using neutron scattering at a displacive structural phase transition find it to be resolution limited at all temperatures above T_c. Our results suggest that an upper resolution limit of 0.02 THz (FWHM) is appropriate for the central peak in the three compounds considered here, and we conclude that substitutional impurities do not affect the energy width. A resolution-limited peak is consistent with the idea of Axe *et al* (1974) that

the strain field surrounding an impurity stabilises the low temperature structure and introduces a Bragg-like component into the scattering. However, the intensity of the central peak in the disordered crystals is not significantly enhanced over that in pure $KMnF_3$. This may be because substitutional impurities probably introduce random bonds into the system which do not necessarily give rise to a quasi-elastic peak above T_c (Halperin and Varma 1976). The experiments are considerably hampered by the overdamped phonon, and it might be instructive to investigate doped $SrTiO_3$ for which the phonon is underdamped above T_c.

5.3. *Comparison of the anomalous scattering observed in the x-ray (I) and neutron experiments*

The anomalous scattering observed in the x-ray (I) and neutron experiments are not immediately comparable since the scattered x-rays automatically integrate over the energy and so include contributions from the phonon and the central peak at all wavevectors. Also, since neutrons with different energy transfers will have different wavevector transfers, the integrated intensity of the scattering measured in the two cases cannot be directly compared. However, both the central peak and the x-ray component have been associated with the presence of defects, so experiments of the two types on the same crystals should enable some comparison to be made. A potential source of error is clustering of defects, since x-rays only illuminate a small part of the crystal while the entire crystal volume is bathed in a neutron beam. This problem has been neglected because the x-ray component is well described by a model based on isolated random fields, and the results were approximately reproducible when a different portion of the crystal was illuminated. Also, the effect of the surface on the x-ray scattering results has been disregarded because of previous experiments (Ryan *et al* 1986, Nicholls and Cowley 1987, Gibaud *et al* 1987a, b, Nelmes *et al* 1988).

The x-ray scattering experiments (I) show that the substitution of Mg impurity ions for Mn ions in $KMnF_3$ tends to decrease the x-ray central component, while the neutron scattering experiments are less conclusive, but suggest that the neutron central peak is not significantly enhanced by such a substitution. The high resolution measurements indicate that though the temperature dependence of the anomalous scattering observed in the two experiments is similar in both disordered samples (compare figure 7, companion paper, with figure 5) the temperature range over which they are visible is very different. The x-ray component has a very low intensity in the disordered crystals at a reduced temperature of $t = 0.01$, while the neutron central peak persists over a temperature range which is a factor of ten greater, to a reduced temperature of $t = 0.1$. It could be argued that in the high-resolution x-ray scattering experiments (I) the intensity of the x-ray beam is insufficient for the component to be observed at higher temperatures. However, further evidence is provided by the results of fits to the data collected with the low resolution configuration in the two experiments. The cross-over temperatures below which the anomalous x-ray component carries more weight than the phonon (see figure 6 in I) all lie within ten degrees of the respective transition temperatures: such a cross-over is not observed in the neutron results, but the central peak amplitude is first observed some twenty-five degrees above the transition (figure 4).

We therefore conclude that although both the x-ray (I) and neutron anomalous components in $KMnF_3$ are influenced by the impurities present, they probably have a different origin. In particular, the x-ray component (I) is only predicted at a first order

phase transition (Imry and Wortis 1979) and so might be expected to decrease if the transition becomes more continuous, while the neutron central peak has been observed in many continuous phase transitions (most notably in $SrTiO_3$; see Shapiro *et al* (1972)) and is apparently independent of the character of the transition.

6. Summary

The influence of point defects on the R-point structural instability in $KMnF_3$ has been studied using x-ray (I) and neutron scattering. The x-ray scattering results (I) indicate firstly, that substitutional impurities alter the character of the transition and that above a small threshold concentration the transition is continuous (see Cox *et al* 1988). Secondly, they show that for sufficiently high temperatures above the transitions the effect of the impurities is minimal, the wavevector dependence of the critical scattering in the three samples $KMnF_3$, $KMn_{0.99}Mg_{0.01}F_3$ and $KMn_{0.9}Mg_{0.1}F_3$ being well described by the anisotropic Lorentzian model as expected, with the same anisotropy parameters, and giving identical values for the inverse correlation length and static susceptibility. The neutron scattering measurements of the spectral response show that substitutional impurities in $KMnF_3$ increase the damping constant, and hence narrow the already overdamped phonon scattering. The same anisotropy parameters as used in the x-ray analysis were found to describe the dynamic response satisfactorily.

Close to the transition temperature anomalous scattering was observed in the disordered crystals in both the x-ray (I) and neutron cross sections in addition to the scattering from the soft-phonon. The central peak in the spectral response first appeared ~20 K above the transition, while the x-ray (I) component was only observed a few degrees above T_c. Both components increased in intensity as T_c was approached, but neither could be said to drive the transition. The energy width of the central peak was resolution-limited in all samples investigated, while the wavevector width of the x-ray component (I) was broader than the resolution and well described by an isotropic Lorentzian squared model. The results suggest that both the components are related to random fields in the system, such as occur when isolated symmetry-breaking impurities are present. We find that the intensity of the components is not significantly enhanced when substitutional impurities are introduced, which may be because such impurities are more likely to introduce random bonds than random fields, and an increase in the concentration of the latter could only occur as a secondary effect.

Acknowledgments

We are indebted to the Institut Laue–Langevin, Grenoble for the use of the neutron scattering facilities, and to Dr R C C Ward for growing the crystals. We have benefitted from helpful discussions with Professor R A Cowley, and from the technical support of R Arthand. Financial support was provided by SERC, and one of us (UJC) is grateful for an SERC studentship.

References

Axe J D, Shapiro S M and Shirane G 1974 *Anharmonic Lattices, Structural Transitions and Melting* ed. T Riste (Leiden: Noordhoff) p 23

Bruce A D and Cowley R A 1980 *Adv. Phys.* **29** 219
Cox U J 1989 *J. Phys: Condens. Matter* **1** 3565–77
Cox U J, Gibaud A and Cowley R A 1988 *Phys. Rev. Lett.* **61** 982
Gesi K, Axe J D, Shirane G and Linz A 1972 *Phys. Rev.* B **5** 1933
Gibaud A, Ryan T W and Nelmes R J 1987a *J. Phys. C: Solid State Phys.* **20** 3833
Gibaud A, Cowley R A and Mitchell P W 1987b *J. Phys. C: Solid State Phys.* **20** 3849
Halperin B I and Varma C M 1976 *Phys. Rev.* B **14** 4030
Hastings J B, Shapiro S M and Frazer B C 1978 *Phys. Rev. Lett.* **40** 237
Imry Y and Wortis M 1979 *Phys. Rev.* B **19** 3580
Kjems J K, Shirane G, Müller K A and Scheel H J 1973 *Phys. Rev.* B **8** 1119
Nicholls U J and Cowley R A 1987 *J. Phys. C: Solid State Phys.* **20** 3417
Nelmes R J, Hatton P E and Vass H 1988 *Phys. Rev. Lett.* **60** 2172
Ryan T W, Nelmes R J, Cowley R A and Gibaud A 1986 *Phys. Rev. Lett.* **56** 2704
Shapiro S M, Axe J D, Shirane G and Riste T 1972 *Phys. Rev.* B **6** 4332